Microbiome

RESEARCH

Open Access

Maternal intestinal *L. vaginalis* facilitates embryo implantation and survival through enhancing uterine receptivity in sows

Qianhong Ye[1,2,3], Yifan Hu[1,2,3], Haoyi Jiang[1,2,3], Tingting Luo[1,2,3], Longshan Han[1,2,3], Yuwen Chen[1,2,3], Jiaying Chen[1,2,3], Libao Ma[1,2,3], Ziyi He[1,2,3] and Xianghua Yan[1,2,3,4*]

Abstract

Background The embryo implantation quality during early pregnancy is the predominant factor for embryo survival and litter performance in sows. Gut microbiota is demonstrated to show a correlation to pregnancy outcomes by participating in regulating maternal metabolism. However, the specific functional microbiota and its mechanical effects on regulating embryo implantation and survival remain unclear. The objective of this study was to clarify whether embryo implantation and litter performance were affected by maternal intestinal microbiota, and to identify specific microbial communities and its mechanism in regulating embryo implantation.

Results In this study, we first conducted 16S rRNA sequencing and metabolomic analysis revealing the intestinal microbiota and metabolism of 42 sows with different litter size to select the potential functional microbiota that may contribute to embryo survival. Then, we explored the effects of that microbiota on embryo implantation and litter performance through microbiota transplantation in mice and sows. We found that maternal intestinal *L. vaginalis* exhibits enrichment in sows with higher litter size, which could facilitate embryo implantation and survival and ultimately increases litter size in mice. We further employed transcriptomic analysis to determine the characteristics of uterus, which found an enhanced uterine receptivity after *L. vaginalis* gavage. The plasma untargeted metabolomic analysis after *L. vaginalis* gavage in mice and targeted metabolomics analysis of in vitro cultured medium of *L. vaginalis* were used to evaluate the metabolic regulation of *L. vaginalis* and to reveal the underlying functional metabolites. Next, an increasing adhesion rate of endometrial-embryonic cells and an obvious increasing formation of pinopodes in cell surface of porcine endometrial epithelial cells were observed after treatments of *L. vaginalis* metabolites, especially galangin and daidzein. Also, the gene expression levels related to uterine receptivity were increased after treatments of *L. vaginalis* metabolites in porcine endometrial epithelial cells. Finally, we found that *L. vaginalis* or its metabolites supplementation during early gestation significantly increased the litter performance in sows.

Conclusions Overall, intestinal microbial-host interactions can occur during early pregnancy and may be contribute to maternal metabolic changes and influence pregnancy outcomes in mammals. Our study provides insights of maternal intestinal *L. vaginalis* to enhance uterine receptivity and to benefit embryo/fetal survival through a gut-uterus axis, contributing to advanced concept and novel strategy to manipulate gut microbiota during early pregnancy, and in turn to improve embryo implantation and reduce embryo loss in sows.

Keywords Embryo implantation, Uterine receptivity, *L. vaginalis*, Litter performance, Sows

*Correspondence:
Xianghua Yan
xhyan@mail.hzau.edu.cn
Full list of author information is available at the end of the article

Introduction

Reproductive performances, especially litter performances of multiparous animals and pregnancy outcomes of uniparous animals, are impacted by many factors, such as genetic inheritance, food, environment, and management. Litter performance including litter size (number of pups born) and live litter size (number of pups born alive) are traits with low heritability, which is estimated to be nearly 0.1 in pigs [1]. Therefore, appropriate regulation of maternal nutritional metabolic status can be a considerable efficient way to facilitate embryo development and survival [2]. Embryo implantation quality is the predominant factor for embryo survival and litter performance, as embryo loss most occurs during peri-implantation period in mammals [3, 4]. Recent years, with the continuous maturity of assisted reproduction technology including in vitro fertilization and embryo transfer, the quality of early embryo development and the embryo preparation have been effectively improved, rendering the uterine receptivity become a key factor restricting the smooth implantation of embryos into the uterus [5]. Altered uterine receptivity, which can be caused by a poor-receptive endometrium or a shifted receptive window, will contribute to embryo implantation failure or poor implantation quality and efficiency, and then lead to embryo loss including fetal development delay, malformation, miscarriage, stillbirth, or preterm birth [6, 7].

Gut microbiota is demonstrated existing correlation effects to fetal development by participating in regulating maternal metabolism and interacting with host signaling pathways [8, 9]. Notably, the abundance of microbiota in the gastrointestinal tract exceeds the number of host cells by 10 times in humans, with bacteria making up the majority and colon containing 70% of the body's microbiota [10]. Changes in the composition and abundance of intestinal microbiota, as well as their metabolites' translocation to brain, ovaries, uteri, and placenta during pregnancy, may alter the maternal reproductive endocrine system and regulate epigenetic modifications of embryonic development and fetal physiology [9, 11, 12]. Therefore, dietary intervention with functional probiotics and prebiotics may ameliorate or prevent the development of metabolic syndrome, while improving pregnancy outcomes in mammals [8, 13, 14]. However, the specific functional microbiota and its mechanical effects on regulating embryo implantation and survival remain unclear.

Based on the emerging link between the microbiota and reproduction [2, 9, 11], we aimed to determine whether and how embryo implantation and survival is affected by maternal intestinal microbiota, to identify specific microbial communities and investigate its role in improving embryo implantation. The early embryo loss of pigs is the highest among all domestic animals, as about 30–50% of embryos are lost during gestation [3, 15]. As such, improving embryo survival during early gestation could effectively increase the efficiency of pig production and makes pigs as an important model to study embryo implantation and survival. Here, we analyzed the intestinal microbiome of sows with different litter size and selected the potential functional microbiota that may contribute to embryo survival at early gestation. We further explored the effects and underlying mechanisms of that microbiota on litter performance and embryo implantation efficiency through microbiota transplantation in mice. Remarkably, we found that *Lactobacillus vaginalis* (*L. vaginalis*) could effectively improve embryo implantation efficiency and enhance uterine receptivity, which in turn increase the litter size and litter weight in mice. We further revealed the enhancement effects of *L. vaginalis* metabolites (especially galangin and daidzein) on endometrium-embryo adhesion and the formation of pinopode on cell surface of porcine endometrial epithelial cells (PEECs). Finally, we confirmed the important roles of oral administration of *L. vaginalis* or its metabolites during early gestation in promoting litter performances in sows. These results suggest that maternal intestinal microbiota may be powerful modulators in gut-uterus axis and *L. vaginalis* may provide an avenue to improve embryo implantation and combat embryo loss in mammals.

Results

A distinct intestinal microbiota composition in sows with different reproductive performances

To explore the intestinal microbial characteristics in sows with different reproductive performance, we collected and frozen the fresh feces of Landrace × Yorkshire crossbred (L × Y) sows at early gestation and recorded the numbers of total piglets (litter size) and live piglets (live litter size) born at delivery (Fig. 1A). Sows with litter size nearly 15 ~ 21 or 9 ~ 11 were respectively grouped into High L × Y group or Low L × Y group, and both the litter size and live litter size of sows were significantly different in High L × Y group and Low L × Y group (Fig. 1B and C). The concentration of estradiol in High L × Y group was significantly higher than that in Low L × Y group (Fig. 1D). However, the levels of progesterone and SCFAs were not significantly different between High L × Y and Low L × Y groups (Fig. 1E and F).

To dig out the functional bacteria that may influence the embryo survival, we generated fecal 16 s rRNA sequencing analysis in sows with different litter size, and the 16 s rRNA tags (V3-V4) showed a satisfactory sequencing depth of bacterial DNA (Figure S1A). Tags were rarefied and clustered in 3036 ASVs (Figure S1B), and the β-diversity of gut microbiota that showed by

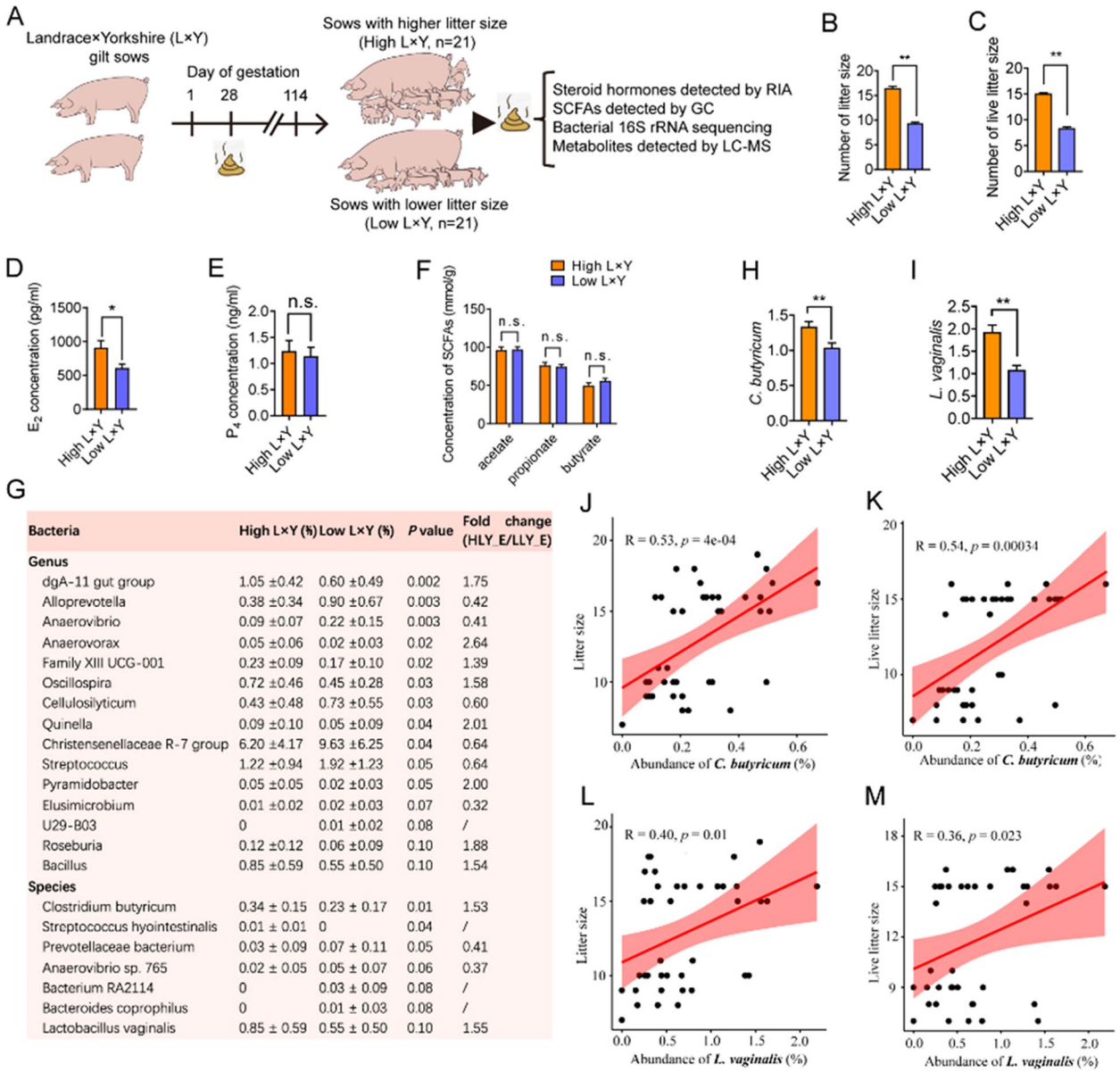

G

Bacteria	High L×Y (%)	Low L×Y (%)	*P* value	Fold change (HLY_E/LLY_E)
Genus				
dgA-11 gut group	1.05 ±0.42	0.60 ±0.49	0.002	1.75
Alloprevotella	0.38 ±0.34	0.90 ±0.67	0.003	0.42
Anaerovibrio	0.09 ±0.07	0.22 ±0.15	0.003	0.41
Anaerovorax	0.05 ±0.06	0.02 ±0.03	0.02	2.64
Family XIII UCG-001	0.23 ±0.09	0.17 ±0.10	0.02	1.39
Oscillospira	0.72 ±0.46	0.45 ±0.28	0.03	1.58
Cellulosilyticum	0.43 ±0.48	0.73 ±0.55	0.03	0.60
Quinella	0.09 ±0.10	0.05 ±0.09	0.04	2.01
Christensenellaceae R-7 group	6.20 ±4.17	9.63 ±6.25	0.04	0.64
Streptococcus	1.22 ±0.94	1.92 ±1.23	0.05	0.64
Pyramidobacter	0.05 ±0.05	0.02 ±0.03	0.05	2.00
Elusimicrobium	0.01 ±0.02	0.02 ±0.03	0.07	0.32
U29-B03	0	0.01 ±0.02	0.08	/
Roseburia	0.12 ±0.12	0.06 ±0.09	0.10	1.88
Bacillus	0.85 ±0.59	0.55 ±0.50	0.10	1.54
Species				
Clostridium butyricum	0.34 ± 0.15	0.23 ± 0.17	0.01	1.53
Streptococcus hyointestinalis	0.01 ± 0.01	0	0.04	/
Prevotellaceae bacterium	0.03 ± 0.09	0.07 ± 0.11	0.05	0.41
Anaerovibrio sp. 765	0.02 ± 0.05	0.05 ± 0.07	0.06	0.37
Bacterium RA2114	0	0.03 ± 0.09	0.08	/
Bacteroides coprophilus	0	0.01 ± 0.03	0.08	/
Lactobacillus vaginalis	0.85 ± 0.59	0.55 ± 0.50	0.10	1.55

Fig. 1 A distinct intestinal microbiota composition in sows with different reproductive performances. **A** Overview of study design for unveiling relationship of maternal intestinal microbiota and reproductive performance in sows with higher or lower litter size. **B**–**C** Number of litter size and liver litter size in sows. **D**–**F** Levels of estradiol (E_2), progesterone (P_4), and short chain fatty acids (SCFAs) in feces of sows at day 28 of pregnancy. **G** Intestinal different bacteria showed in genus and species level between sows with higher and lower litter size. **H**–**I** The abundance of intestinal *C. butyricum* and *L. vaginalis* in sows detected by qRT-PCR. **J**–**M** The scatter plots of correlation coefficient for abundance of *C. butyricum* and *L. vaginalis* correlated with litter size and live litter size. Statistical analyses were performed using unpaired Students' *t*-test (**B**–**F**) or Mann–Whitney *U* test (**G**). ns, not significant; *$p < 0.05$; **$p < 0.01$. **J**–**M** Correlation coefficients were analyzed using Pearson correlation analysis, and least square linear regression lines (red line) with 95% confidence interval (pink shading) are provided for visual representation of the non-parametric testing

PCoA on ASV level demonstrated obvious difference between High L× Y and Low L× Y groups (Figure S1C). However, we found that the α-diversity indices including sobs, chao, ACE, Shannon, Simpson, and coverage were not significantly different in these two groups (Figure S1D). Further taxon analysis showed that the intestinal bacteria of these 42 sows were dominated by two phyla (i.e., Firmicutes and Bacteroidota) (Figure S1E) and 15 genera (Figure S1F). Compared with Low L× Y group, sows in High L× Y group harbored more *dgA-11 gut group*, *Anaerovorax*, *Family XIII UCG-001*, *Oscillospira*, *Quinella*, *Pyramidobacter*, *Roseburia*, and *Bacillus*

in genus level and more *C. butyricum* and *S. hyointestinalis* in species level (Fig. 1G). In addition, the results of linear discriminant analysis effect size (LEfSe) suggested that *C. butyricum* and *S. hyointestinalis* were characteristic bacteria that enriched in sows' gut in High L × Y group (Figure S1G). However, the concentration of intestinal *S. hyointestinalis* was too low in both High L × Y and Low L × Y groups (0.01 ± 0.01% vs 0) (Fig. 1G). Moreover, the abundances of *C. butyricum* and *L. vaginalis* in High L × Y group were both 1.5 times larger than that in Low L × Y group (Fig. 1G). Then, we used qRT-PCR revealing that the abundances of *C. butyricum* and *L. vaginalis* in High L × Y group were significantly higher than that in Low L × Y group (Fig. 1H and I). Importantly, we found that the abundances of *C. butyricum* and *L. vaginalis* were both significantly correlated with the litter size and live litter size of sows (Fig. 1J–M). Therefore, we assumed that *C. butyricum* and *L. vaginalis* were potential functional microbiota in regulating embryo survival and pregnancy outcomes.

Untargeted metabolomics reveals intestinal metabolism changes in sows with different reproductive performances

Metabolic regulation could play important roles in microbiota regulating reproduction in mammals, but the mechanisms through which maternal gut microbiota might influence intestinal metabolism and consequently embryo development have not yet been fully understood. We determined the intestinal metabolites profiling using untargeted metabolomics and the partial least squares discriminant analysis (PLS-DA) showed that the detected metabolites had a distinct signature between High L × Y and Low L × Y groups (Fig. 2A). A total of 3172 metabolites were detected, with 37 metabolites were significantly higher and 60 metabolites were significantly lower in High L × Y group than that in Low L × Y group (Fig. 2B). The expression profile and variable importance in the projection (VIP) of different metabolites were showed in Figure S2, and the enrichment of these different metabolites demonstrated that linoleic acid metabolism was the major pathway, followed with retinol metabolism, arginine biosynthesis, pyrimidine metabolism, arachidonic acid metabolism, thiamine metabolism, aminoacyl-tRNA biosynthesis, and taurine and hypotaurine metabolism (Fig. 2C). A correlation analysis was conducted among the abundances of intestinal different metabolites and the bacteria including *C. butyricum* and *L. vaginalis*, as well as litter sizes of sows. The results showed that the litter sizes and abundances of *C. butyricum* and *L. vaginalis* had a similar correlation pattern to these metabolites (Fig. 2D). Among these metabolites, nirvanol showed a significant positive correlation, but linoleic acid and 4β-hydroxystanozolol showed a significant negative correlation to the litter sizes and abundance of *C. butyricum* and *L. vaginalis* (Fig. 2D).

Microbiota transplantation of *L. vaginalis* improves embryo implantation and increases litter sizes in mice

Using microbiota transplantation, we aimed to investigate the effects of *C. butyricum* and *L. vaginalis* on embryo implantation and survival. As shown in Fig. 3A, *C. butyricum* and *L. vaginalis* were gavaged alone or in combination from pre-breeding to early pregnancy in mice. Firstly, we found that the total litter size, live litter size, and total litter weight were significantly increased after *L. vaginalis* transplantation alone or mixed with *C. butyricum* (Fig. 3B–D). However, *C. butyricum* transplantation alone had no significant effects on total litter size, live litter size, and total litter weight (Fig. 3B–D). In addition, the average litter pups' weight and coefficient of variation (CV) of litter pups' weight were not significantly influenced after *C. butyricum* and *L. vaginalis* gavage alone or in combination (Fig. 3E–F). Moreover, the ratio of male was increased, but the ratio of female was decreased in litter pups after *C. butyricum* or *L. vaginalis* transplantation (Fig. 3G-H). Given the fact that the quality of embryo implantation determines the pregnancy outcomes [16, 17], we hypothesized that the improved litter performance induced by *L. vaginalis* transplantation may result from the benefits of embryo implantation. To further identify this speculation, the number of implantation sites in uterus and embryo survival rate (embryo implantation efficiency) was investigated. We found that the number of embryo implantation sites and the embryo survival rate were increased after *L. vaginalis* transplantation alone or mixed with *C. butyricum* (Fig. 3I–J). However, there were no effects on the number of embryo implantation sites but had an increasing tendency to improve the embryo survival rate induced by *C. butyricum* transplantation alone (Fig. 3I–J). In addition, the number of corpus luteum in ovaries was not significantly influenced after *C. butyricum* and *L. vaginalis* gavage alone or in combination (Fig. 3K). Overall, this leads to hypothesis that *L. vaginalis* is a key intestinal microbe to benefit embryo implantation and survival during early pregnancy, subsequently to increase the litter size and litter weight.

To decipher the effective components affecting embryo implantation and survival in microbiota transplantation test, we separated the bacteria cells (LV_B) and extracellular metabolites (LV_M) of *L. vaginalis* after its in vitro culture for 30 h and then evaluated the embryo survival rate after gavage of LV_B or LV_M in mice (Fig. 3L). We find that gavage of LV_B or LV_M could both increase the number of implantation sites and embryo survival rate (Fig. 3M and N), whereas the

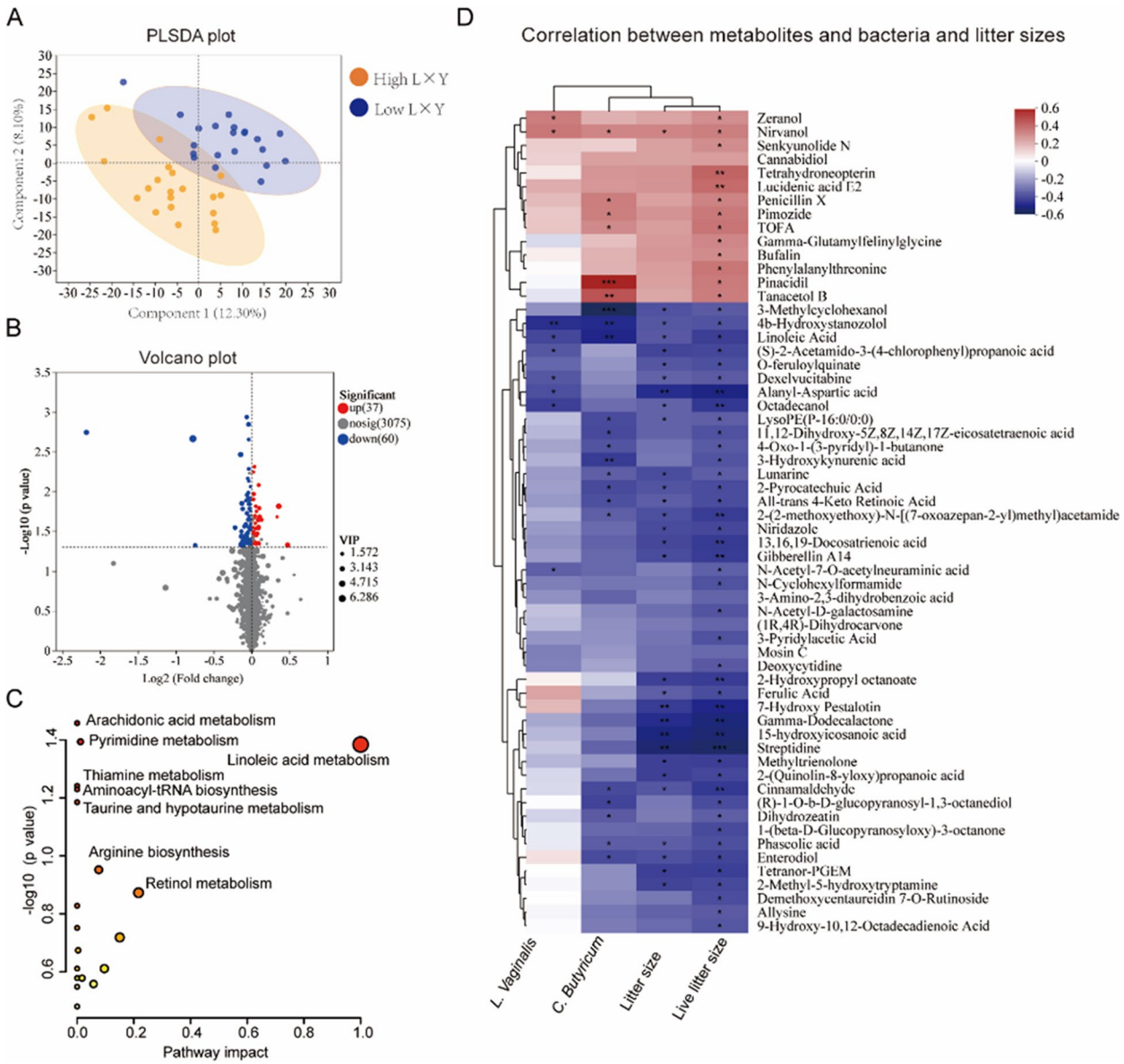

Fig. 2 Untargeted metabolomics analysis reveals intestinal metabolism changes in sows with different reproductive performances. **A**–**B** PLS-DA analysis and volcano plot (High L × Y group vs Low L × Y group) of fecal metabolome of sows at day 28 of pregnancy. **C** Pathway enrichment analysis of different metabolites. The color gradients and circles' size respectively correspond to the fluctuation of -log10 (*p* value) and impacts. **D** Correlation between intestinal different metabolites and bacteria and litter size. Correlation coefficients were analyzed using Spearman correlation analysis. $n = 21$

number of corpus luteum was unchanged compared with PBS or MRS groups (Fig. 3O). Importantly, we collected and identified the in vitro cultured metabolites of *L. vaginalis* after its culture for 0, 4, 12, and 30 h according to the growth curve (Fig. 4A). The PCA plot suggested that the metabolic patterns were similar between 0 and 4 h, but that patterns were different to 12 h and 30 h (Fig. 4B). Among these, the metabolic pattern at 30 h showed most difference compared with the other three groups (Fig. 4B). The substrates and products of *L. vaginalis* could be effectively located according to the concentration heatmap (Fig. 4C) and multiple changes of metabolites (Fig. 4D). The trend analysis plots revealed the dynamic changes of metabolites' concentrations under different times, which further estimated the substrates and products of *L. vaginalis* (Figure S3). Notably, the different metabolites including substrates and products of *L. vaginalis*

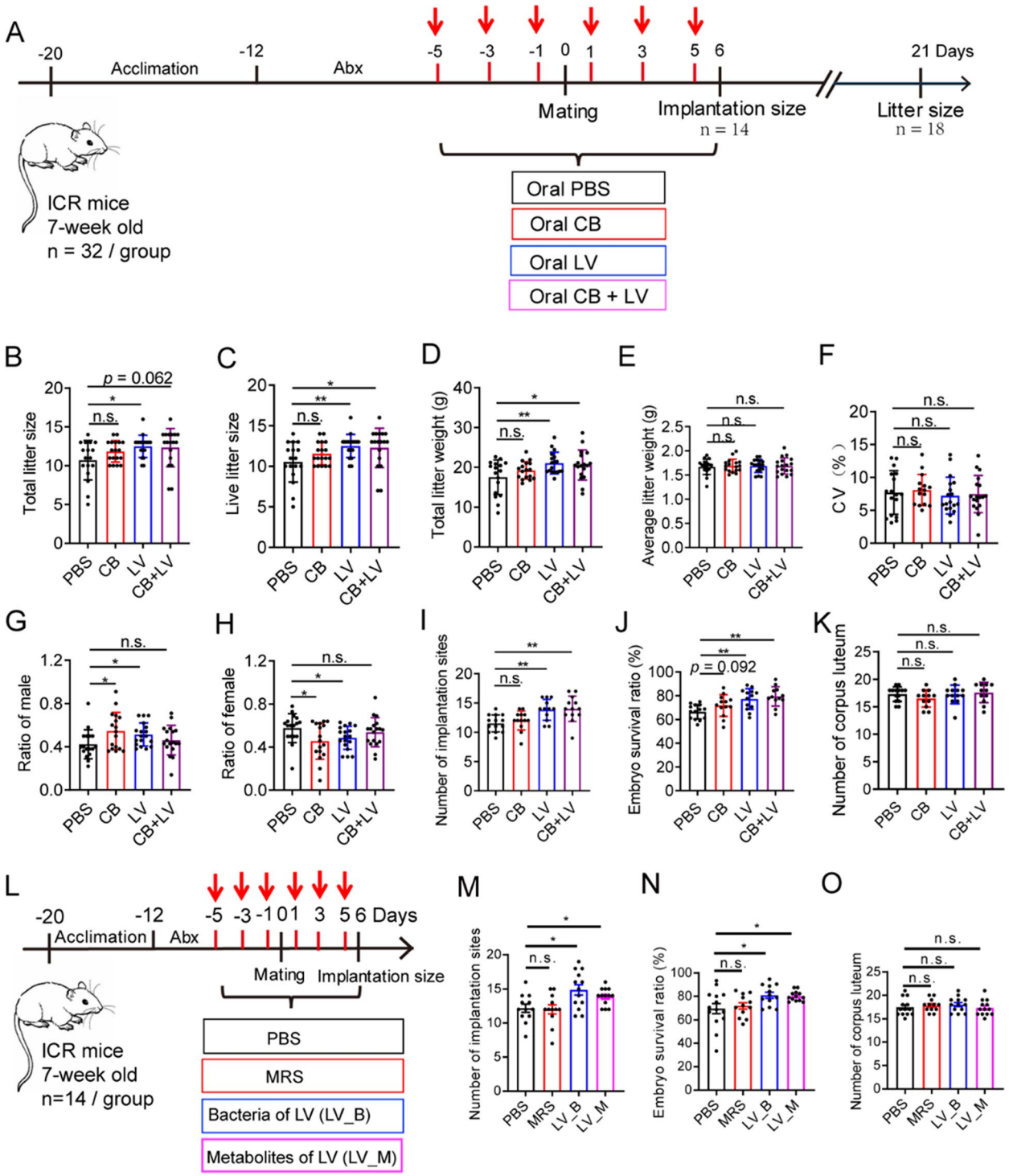

Fig. 3 Microbiota transplantation of *L. vaginalis* improves embryo implantation and increases litter sizes in mice. **A** Experimental scheme for the generation and analysis of microbiota transplantation on embryo implantation efficacy at early pregnancy and offspring survival at delivery. **B**–**H** The total litter size, live litter size, total litter weight, average litter weight, coefficient of variation of litter pups' weight, and the ratios of male or female of litter pups at delivery after microbiota transplantation in mice. **I**–**K** Number of embryo implantation sites, embryo survival ratio, and number of corpus luteum at day 6 of pregnancy. **L** Experimental scheme for the generation and analysis of bacterial cells or metabolites of *L. vaginalis* supply on embryo implantation efficacy. **M**–**O** Number of embryo implantation sites, embryo survival ratio, and number of corpus luteum at day 6 of pregnancy in mice after bacterial cells or metabolites of *L. vaginalis* supply. In A and L, the red arrow points to the date of gavage. Statistical analyses were performed using unpaired Students' *t*-test. ns, not significant; $*p < 0.05$; $**p < 0.01$

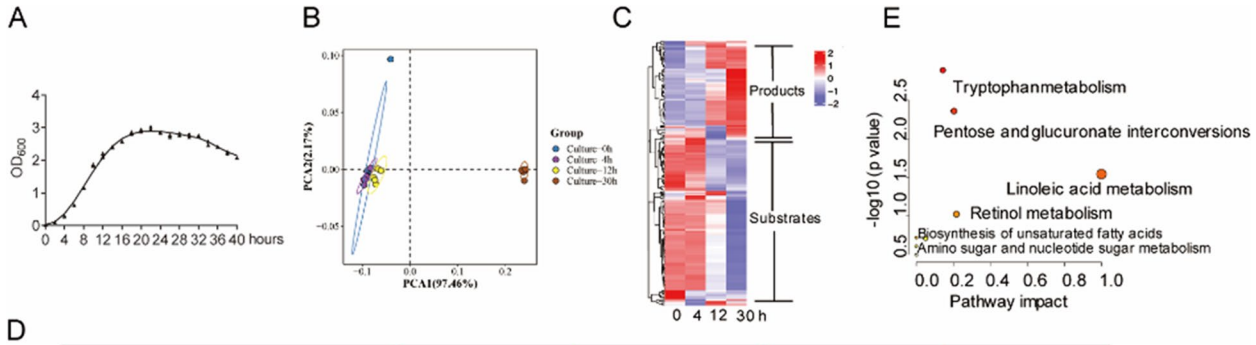

D

Metabolites	FC (0 h VS 30 h)	FC (4 h VS 30 h)	FC (12 h VS 30 h)	Levels of 30 h
Quinaldic acid	180.97	23.44	2.44	4.14
all-trans-Retinoic acid	164.99	11.51	79.47	8.35
Phenyllactic acid	42.84	5.30	n.s.	107.78
10Z-Nonadecenoic acid	42.43	13.08	12.78	61.23
Hydroxyphenyllactic acid	26.06	20.55	2.32	17.09
D-Xylulose	20.45	8.14	1.95	49.05
Ricinoleic acid	17.78	6.47	12.81	14.58
2-hydroxy-4(methylthio) Butanoate	16.16	7.88	1.45	48.69
Phenylglyoxylic acid	16.08	7.87	1.45	33.22
Sulindac	14.56	6.56	n.s.	66.14
4-Hydroxyphenyl-2-propionic acid	10.96	3.93	n.s.	151.25
Idoxuridine	10.07	6.86	n.s.	0.94
L-3-Phenyllactic acid	7.50	3.34	n.s.	107.78
Xanthurenic acid	7.13	5.67	1.98	8.49
3-Indolebutyric acid	6.55	5.25	1.59	1.53
D-Xylose	3.60	3.32	n.s.	449.13
N-acetyl-D-glucosamine	3.36	3.04	n.s.	54.48
Indoleacetic acid	2.95	2.38	n.s.	458.21
Indolepyruvate	2.73	2.44	1.79	3.27
Xanthosine	2.72	2.26	n.s.	0.36
p-Hydroxymandelic acid	2.61	2.53	2.28	1.09
3-Indoleethanol	2.54	2.17	n.s.	56.87
L-Tryptophan	2.53	2.39	1.62	1494.84
Linolelaidic acid	2.53	2.09	15.44	17.95
Quinic acid	2.51	2.27	2.70	43.22
Hexanoylcarnitine	2.50	2.22	n.s.	1208.66
beta-Glycerophosphoric acid	2.37	3.08	n.s.	4.93
3,6-Diketocholanic acid ethyl ester	2.26	1.96	11.07	6.61
6-Methyladenine	2.21	2.46	2.24	0.56
N-Acetylglutamine	2.17	1.94	n.s.	73.20
23-Norcholic acid	2.12	1.94	n.s.	3.71
D-Arabinose	2.11	2.22	1.55	329.72

Fig. 4 Targeted metabolomics analysis exhibits ex vivo cultured metabolites of *L. vaginalis*. **A** Growth curve of *L. vaginalis* measured by turbidimetric method. **B** PCA analysis of targeted metabolome of *L. vaginalis* ex vivo cultured for 0, 4, 12, and 30 h. **C** Heatmap of metabolites showing products and substrates of *L. vaginalis*. **D** Fold changes and levels of metabolites after *L. vaginalis* cultured for 30 h. **E** Pathway enrichment analysis of different metabolites (30 h vs 0 h) of *L. vaginalis*. $n = 6$

was most enriched to tryptophan metabolism, pentose and glucuronate interconversions, linoleic acid metabolism and retinol metabolism (Fig. 4E), which were partially consistent with the intestinal enrichment pathways in sows between High L × Y and Low L × Y groups (Fig. 2C).

Microbiota transplantation of *L. vaginalis* promotes uterine receptivity and modulates plasma metabolism in mice

To further explore the potential mechanisms of *L. vaginalis* in regulating embryo implantation, the histomorphology of uterine implantation site and colon tissue was observed, and the microbiota composition in colon,

ovarian steroid hormones synthesis, uterine receptivity, and metabolic changes in plasma were also investigated. At day 6 of pregnancy, the gestational sac and decidualized tissue can be clearly observed in both groups, and the colon biopsy showed that the colonic morphology was not affected after *L. vaginalis* gavage

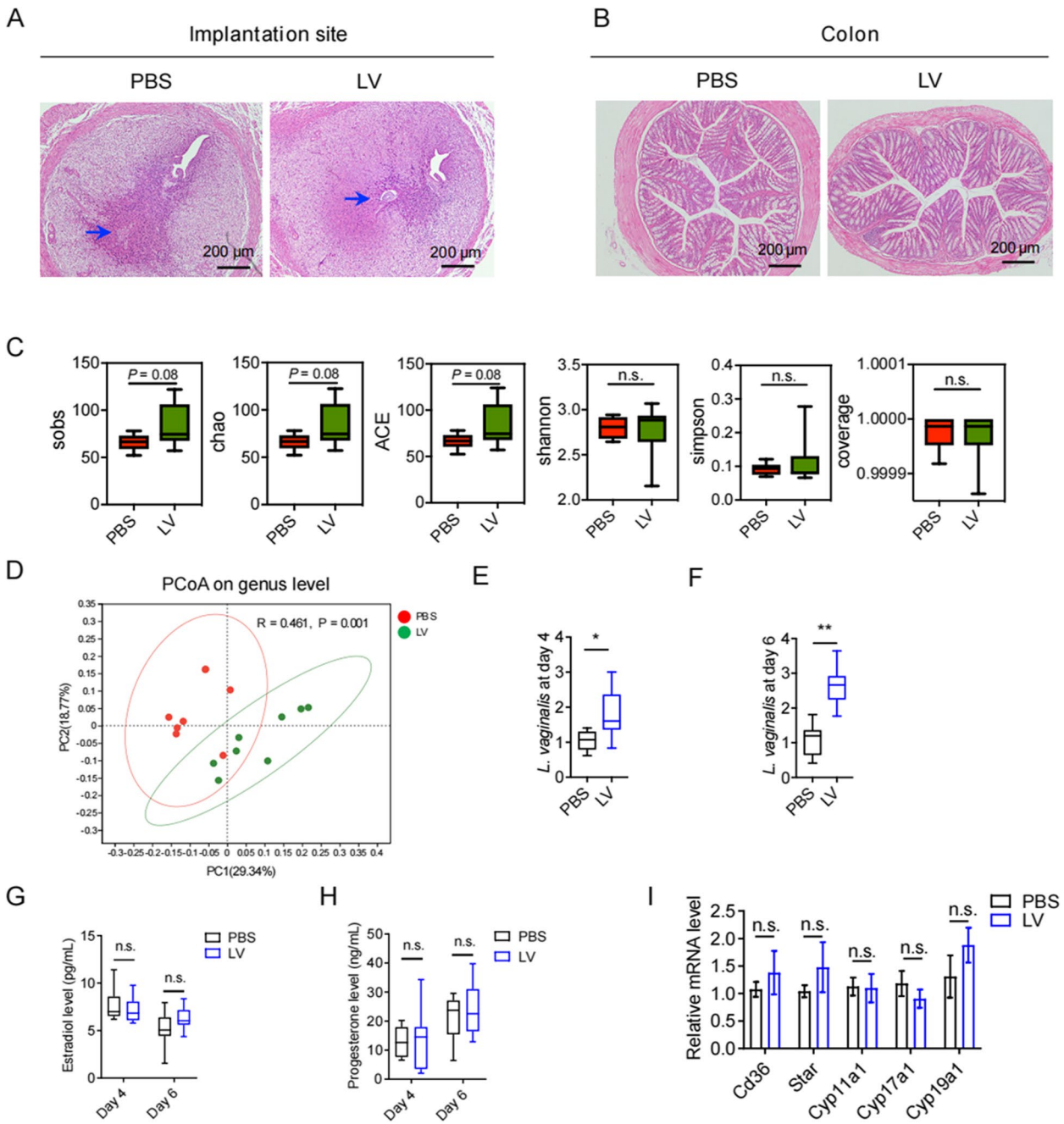

Fig. 5 Effects of *L. vaginalis* transplantation on histomorphology of uterus and colon, colonic microbiota composition, and steroid hormones synthesis in mice. **A**–**B** Representative H&E-stained sections of uterine implantation site and colonic tissue of mice at day 6 of pregnancy. The gestational sac was marked with blue arrows. **C** α-diversities of colonic bacteria of mice at day 6 of pregnancy. **D** Colonic microbial communities clustered using PCoA of weighted Unifrac matrix. **E**–**F** The abundance of *L. vaginalis* detected by qRT-PCR in colon of mice at day 4 and day 6 of pregnancy. **G**–**H** Levels of estradiol and progesterone in plasma of mice at day 4 and day 6 of pregnancy. **I** The relative mRNA level of genes related to steroid hormones synthesis in ovaries of mice at day 4 of pregnancy. Statistical analyses were performed using Mann–Whitney *U* test (**C**) or unpaired Students' *t*-test (**F**–**H**). ns, not significant; *$p < 0.05$; **$p < 0.01$

(Fig. 5A and B). In addition, the colonic microbiota analysis suggested that the α-diversity including sobs, chao, and ACE had an increasing trend, but Shannon, Simpson, and coverage were not influenced after *L. vaginalis* gavage (Fig. 5C), and the β-diversity analysis showed obvious difference between PBS and *L. vaginalis* gavage (Fig. 5D). Moreover, we found that the abundances of *L. vaginalis* in colon of mice at day 4 and day 6 of pregnancy were significantly increased after *L. vaginalis* gavage (Fig. 5E and F). Steroid hormones including estradiol and progesterone are master regulators of embryo implantation, which coordinate endometrial proliferation and differentiation, and regulate the uterine receptivity [16, 17]. However, we found that the concentrations of plasma estradiol and progesterone were not influenced both at day 4 and day 6 of pregnancy (Fig. 5G and H), additionally, the relative mRNA level of genes related to steroidogenesis including Cd36, Star, Cyp11a1, Cyp17a1, and Cyp191a1 in ovaries at day 4 of pregnancy was unchanged after *L. vaginalis* gavage (Fig. 5I), suggesting that the benefits of *L. vaginalis* in improving embryo implantation and survival were less likely taken action through regulating ovarian steroidogenesis.

To investigate whether the beneficial effects of *L. vaginalis* on embryo survival was due to promoting uterine receptivity, we performed uterine transcriptome analysis, which demonstrated 420 genes upregulated and 96 genes downregulated after *L. vaginalis* transplantation (Fig. 6A). Importantly, embryonic skeletal system development was the most affected pathway enriched

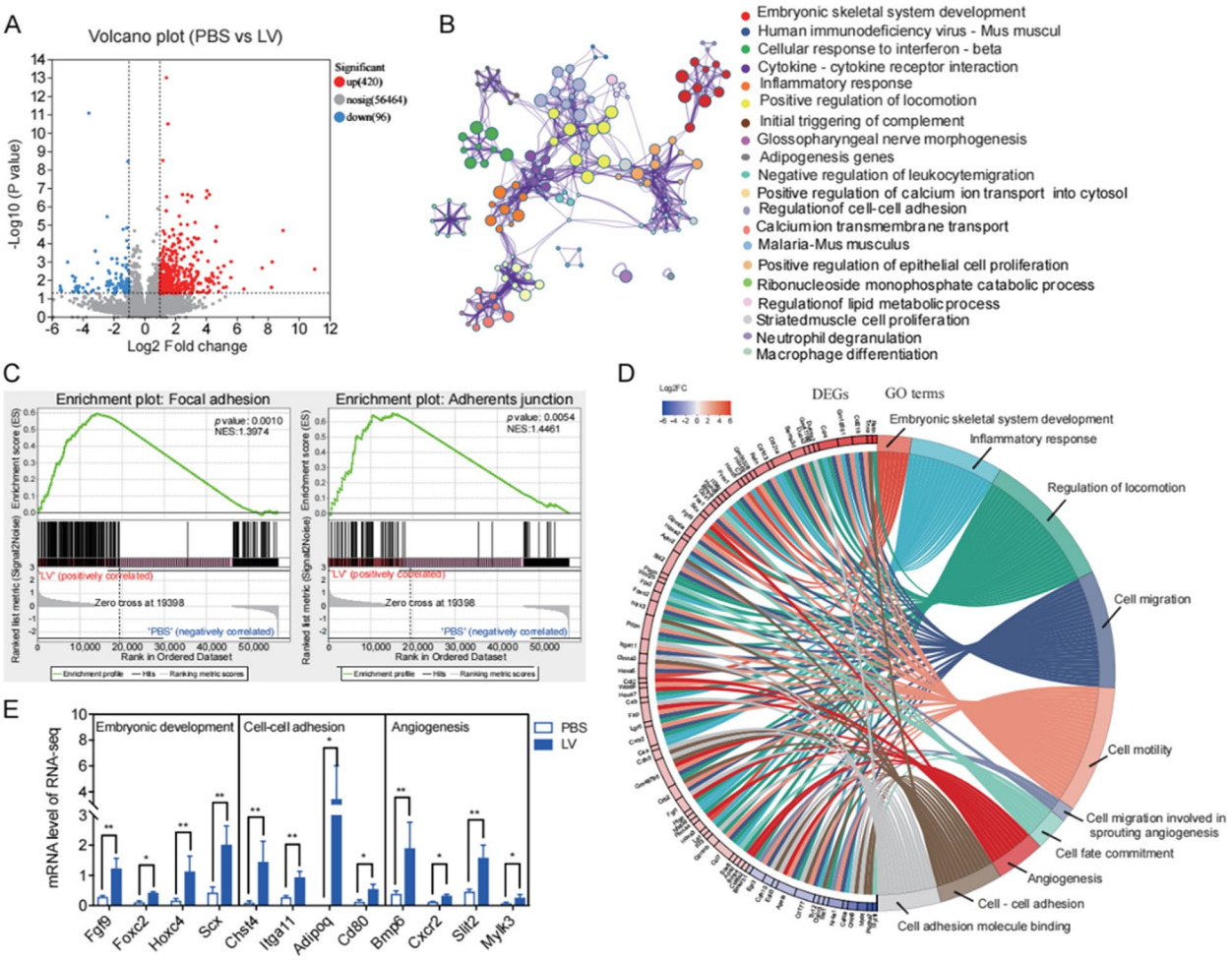

Fig. 6 Microbiota transplantation of *L. vaginalis* enhances uterine receptivity. **A** Volcano plot showing different expressed genes (DEGs) in uterus of mice at day 4 of pregnancy. **B** Network plot showing the subset of enriched GO terms in the top 20 clusters. **C** GSEA analysis showing enriched KEGG pathways related to cell–cell adhesion. **D** Circos plot visualizing putative relationship between DEGs and GO terms. **E** Bar plot showing mRNA level of genes related to embryonic development, cell–cell adhesion, and angiogenesis. Statistical analyses were performed using unpaired Students' *t*-test. *$p < 0.05$; **$p < 0.01$. $n = 4$

by different expressed genes (DEGs), followed by cellular response to interferon-beta, inflammatory response, positive regulation of locomotion, adipogenesis, regulation of cell–cell adhesion, and regulation of lipid metabolic process (Fig. 6B). Moreover, the GSEA results also demonstrated significant enrichment plots included focal adhesion and adherents junction (Fig. 6C). To further identify the specific DEGs responsible for the enriched GO terms including embryonic skeletal system development, cell–cell adhesion, angiogenesis, cell fate commitment, inflammatory response, regulation of locomotion, cell migration and motility, chord plot was employed to exhibit the connection of genes and GO terms (Fig. 6D). Among these, an increased expression level of DEGs related to embryonic development, cell–cell adhesion, and angiogenesis were displayed in Fig. 6E.

In light of the important regulatory roles of metabolic status on genes expression and body homeostasis, we focused on subsequent metabolites profiling in plasma. The PLSDA plot showed that the metabolic pattern of *L. vaginalis* group was significantly different to control group (Fig. 7A). The differential abundance score showed that the most enriched KEGG pathways including GnRH signaling pathway, arachidonic acid metabolism, primary bile acid biosynthesis, linoleic acid metabolism, taurine and hypotaurine metabolism, ovarian steroidogenesis, bile secretion, regulation of lipolysis in adipocytes, aldosterone synthesis and secretion, and retrograde endocannabinoid signaling (Fig. 7B). A joint analysis of plasma metabolome and uterine transcriptome was performed and suggested common enriched pathways including neuroactive ligand-receptor interaction, glycerophospholipid metabolism, alpha-linolenic acid metabolism, linoleic acid metabolism, arachidonic acid metabolism, steroid hormone biosynthesis, retrograde endocannabinoid signaling, aldosterone synthesis and secretion, and regulation of lipolysis in adipocytes (Fig. 7C). Notably, according to the expression profile and VIP of different metabolites displayed in Fig. 7D, we selected the top 5 metabolites including norizalpinin (also known as galangin), norethindrone oxime, taurocholic acid (TCA), daidzein, and caproic acid that not only had higher VIP scores, but also exhibited higher AUC values (Fig. 7E), for subsequent experiments to verify the effects of *L. vaginalis* metabolites on endometrial epithelial cells receptivity in vitro.

L. vaginalis metabolites enhance endometrial epithelial cells receptivity and improve litter performances in sows

Porcine endometrial epithelial cells (PEECs) and porcine iliac artery endothelial cells (PIECs) were used to establish ex vivo cultured endometrium, and then porcine trophoblast cells (PTCs) were added to simulate endometrial-embryo cell adhesion (Fig. 8A and B). After treatments of *L. vaginalis* metabolites including galangin, norethindrone, TCA, daidzein, and caproic acid in endometrium chip for 24 h, we found that galangin and daidzein could markedly motivate the adhesion of PTCs to endometrial epithelium (Fig. 8C). Consistently, we found an obvious increasing formation of pinopodes in cell surface of PEECs after treatments of galangin and daidzein (Fig. 8D). Moreover, the expression level of genes related to uterine receptivity including carbohydrate sulfotransferase 4 (Chst4), integrin subunit beta 3 (Itgb3), bone morphogenetic protein 6 (Bmp6), peroxisome proliferator activated receptor gamma (Pparg), and forkhead box O1 (Foxo1) were detected (Figure S4). The results indicated that TCA increased the expression level of Chst4, Pparg, and Foxo1, caproic acid increased the expression level of Itgb3 and Pparg, daidzein increased the expression level of Bmp6 and Foxo1, and galangin increased the expression level of Foxo1 (Figure S4 A–S4E). Moreover, the expression level of gene, fibroblast growth factor 9 (Fgf9), was examined to exhibit an enhancing expression of Fgf9 after treatments of norethindrone, caproic acid, TCA, and Daidzein, suggesting an improvement effect of *L. vaginalis* metabolites on embryo development (Figure S4 F).

To further verify the effects of *L. vaginalis* on litter performance in sows, oral administration of *L. vaginalis* or its metabolites in sows during early gestation was conducted (Fig. 8E). Notably, the total litter size, live litter size, and litter size of pup's weight higher than 0.95 kg were significantly increased, whereas the average litter pup's weight was not changed after oral administration of *L. vaginalis* and its metabolites (Fig. 8F–I). In addition, the total litter weight was not changed after oral administration of *L. vaginalis* but that was significantly increased after oral administration of the metabolites of *L. vaginalis* (Fig. 8J). Moreover, the abundance of *L. vaginalis* in feces of sows was significantly increased after oral administration of *L. vaginalis* (Fig. 8K).

Discussion

Pregnancy outcomes were demonstrated to be associated with a profound alteration of gut microbiota, which exerts a vital role in maintenance of maternal physiology and fetal development during gestation [11, 12, 18]. Specifically, mounting evidence showed that maternal-microbial metabolites could propel the maturation of neonatal intestinal epithelium and drive the development of offspring's neurophysiology and innate immune system [8, 12, 19, 20]. In addition, compared with sows with lower litter size, sows with higher litter size had a lower diversity of intestinal microbiota and significantly increased insulin resistance and inflammatory

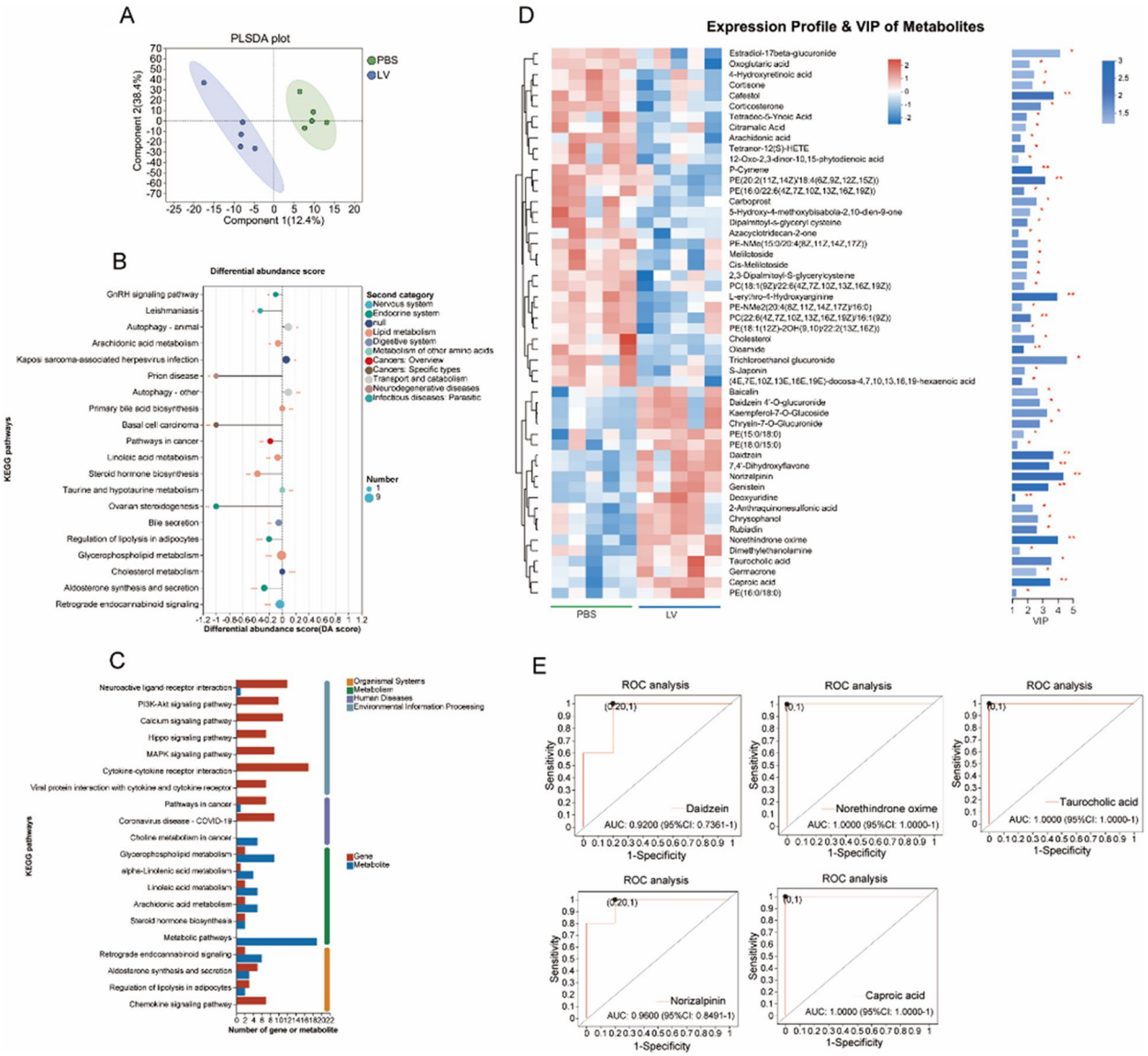

Fig. 7 Microbiota transplantation of *L. vaginalis* modulates maternal plasma metabolism. **A** PLS-DA analysis of plasma metabolome in mice at day 4 of pregnancy. $n = 5$. **B** The differential abundance score (*L. vaginalis* vs PBS) of top 20 enriched KEGG pathways in plasma metabolome analysis of mice at day 4 of pregnancy. **C** Correlation analysis showing the top 20 enriched KEGG pathways for plasma metabolome (blue bar) and uterine transcriptome (red bar) of mice at day 4 of pregnancy. **D** Expression profile and VIP of different metabolites. **E** ROC analysis of different metabolites including daidzein, norethindrone oxime, taurocholic acid, galangin, and caproic acid. Statistical analyses were performed using unpaired Students' *t*-test. $*p < 0.05$; $**p < 0.01$

(See figure on next page.)

Fig. 8 *L. vaginalis* metabolites enhance endometrial epithelial cells receptivity and improves litter performances in sows. **A** Schematic representation of the microfluidic chip used for simulating endometrial-embryo adhesion. **B** Physical photo of the microfluidic chip. **C** Fluorescence microscopy viewing the attachment of PTCs to endometrial microfluidic chip. **D** Scanning electron microscopy viewing the microvilli on the cell surface of PEECs. **E** Experimental scheme for the generation and analysis of bacterial cells or metabolites of *L. vaginalis* supply during early gestation on offspring survival in sows. **F**–**J** Litter performance including total litter size, live litter size, litter size of litter pup's weight higher than 0.95 kg, average litter pup's weight, and total litter weight of sows. **K** The abundance of intestinal *L. vaginalis* in sows detected by qRT-PCR. Statistical analyses were performed using unpaired Students' *t*-test. ns, not significant; $*p < 0.05$; $**p < 0.01$

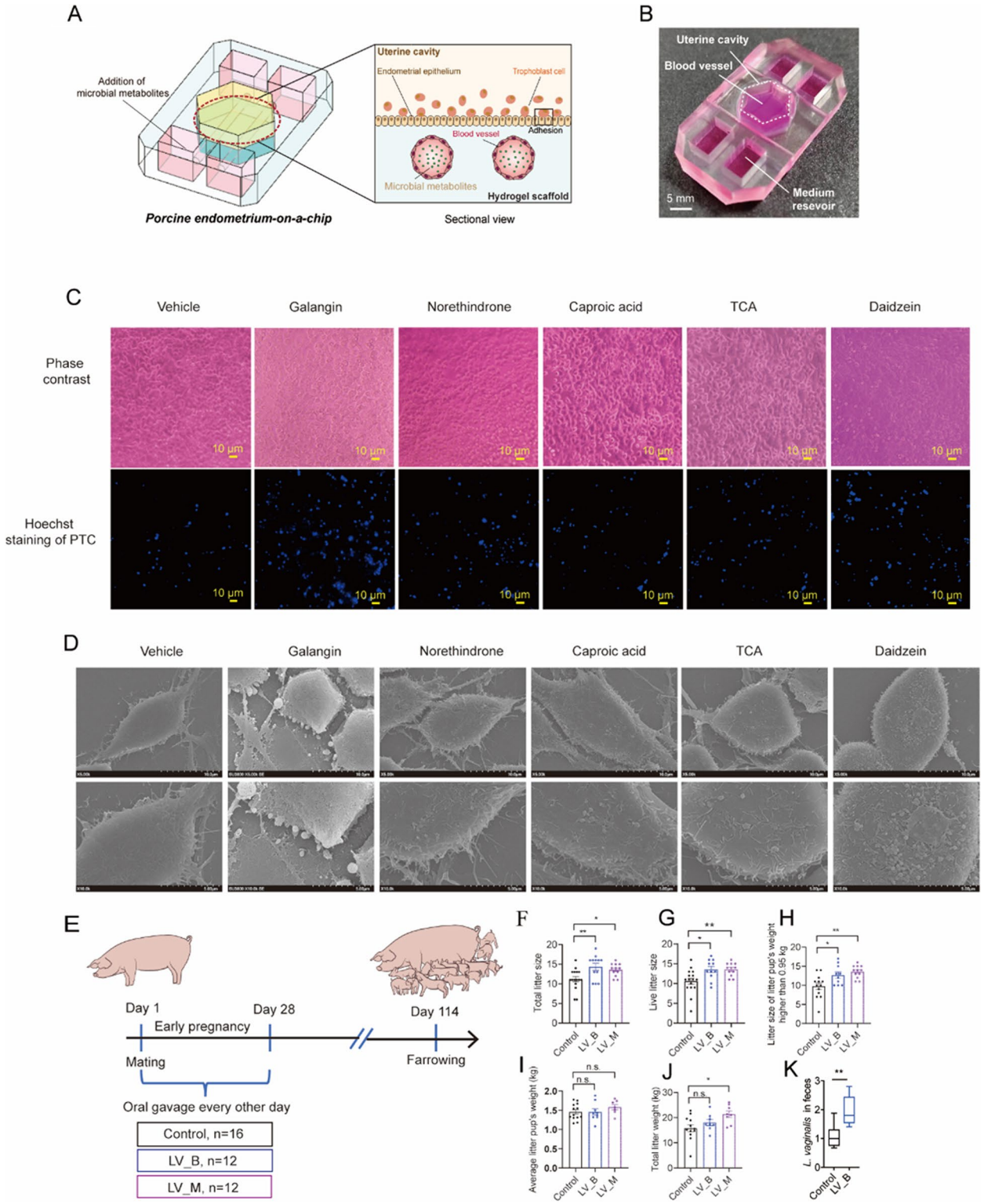

Fig. 8 (See legend on previous page.)

response during late gestation [21]. However, embryo loss most occurs during peri-implantation period at early pregnancy, rendering embryo implantation quality into the predominant factor for embryo survival and litter performance in sows [3]. Therefore, the investigation of whether and how embryo implantation and survival are affected by maternal microbiota is a top priority to understand host-microbiota interactions and could effectively improve litter performance through intestinal microbiota modulation.

Here, we investigated gut microbiota and intestinal metabolism of sows with different reproductive performance and assumed *C. butyricum* and *L. vaginalis* could be potential functional microbiota regulating embryo survival during early gestation. Then, using microbiota transplantation, we assessed the modulation of *C. butyricum* and *L. vaginalis* on embryo survival and pregnancy outcomes, which only found a significant improvement of *L. vaginalis* on embryo implantation efficiency and litter performance in mice. In addition, the plasma metabolomics and uterine transcriptome analysis suggested that *L. vaginalis* could improve embryo implantation through modulating maternal plasma metabolism and promoting uterine receptivity. Furthermore, we selected the key metabolites raised by *L. vaginalis* and identified their regulation on endometrial epithelial cell receptivity, including endometrial-embryonic cells adhesion, the formation of pinopodes in cellular surface of porcine endometrial epithelial cells, and the genes' expression related to uterine receptivity. Notably, we also verified that oral administration of *L. vaginalis* and its metabolites during early gestation could significantly increase the litter performances in sows.

Lactobacillus spp. is considered an optimal cervicovaginal microbiota that associated with favorable health outcomes including lowering rates of preterm birth and reduced susceptibility to sexually transmitted infections in human [22, 23]. In contrast, cervicovaginal microbiota characterized by an increase in anaerobic bacteria and depletion of *lactobacilli* is associated with adverse pregnancy outcomes including low birth weight [24], spontaneous preterm birth [23], and increased risk of acquiring and transmitting infections [25]. Previous studies suggested that lactic acid from vaginal *lactobacillus* could enhance cervicovaginal epithelial barrier integrity by promoting tight junction protein expression [26]. Moreover, *L. vaginalis* BC17 can stimulate the growth of *Bifidobacterium spp.* and exhibit safety for human use [27]. Importantly, in addition to female genital tract, *lactobacillus* most notably colonized at the digestive tract and was identified to maintain intestinal barrier integrity and resist gastrointestinal infection and inflammation [28]. In addition, Zeng et al. recently revealed that *L. vaginalis* exerts hepatoprotective effects during acetaminophen toxicity by liberating daidzein from the diet via β-galactosidase [29]. However, the impacts of intestinal *lactobacillus* on pregnancy outcomes were less investigated. Here, we first found an increased level of intestinal *L. vaginalis* in sows with higher litter size and revealed the improvement effects of *L. vaginalis* on uterine receptivity and embryo implantation efficiency, which ultimately increased the number of litter pups born in sows and mice.

Two principal mechanisms have been proposed for how the gut microbiota can contribute to host physiology: (1) changes dietary nutrients utilization and (2) altered host-microbial interactions that influence the metabolic status [8, 14]. Therefore, we assessed intestinal metabolism and performed correlation analysis with candidate microbiota to assist us acquiring the functional microbiota for improving embryo survival. In addition to the products of bacterial metabolism, gut microbial liberation of bioactive compounds from food that transported into target tissues could also affect host physiology [29, 30]. Hence, we detected the in vitro cultured metabolites of *L. vaginalis* and examined the plasma metabolism in mice after *L. vaginalis* transplantation to locate the key metabolites of *L. vaginalis* in regulating embryo survival. Our data showed that the in vitro cultured products of *L. vaginalis* mainly included lactic acid, short and medium chain fatty acids, bile acid, benzazole, and their derivatives. Additionally, *L. vaginalis* transplantation in mice could remarkably increase the levels of caproic acid, taurocholic acid, and dietary sourced flavonoids and isoflavone. Subsequently, the critical metabolites of *L. vaginalis* influencing embryo survival were located to galangin, norethindrone, and daidzein that could be liberated from the diets, as well as taurocholic acid and caproic acid that could be products of *L. vaginalis* metabolism.

Investigating the embryo implantation process and revealing maternal-embryo interactions in mammals is fundamentally challenging as the implanting embryo is concealed by the uterine tissues. Previously, ex vivo culture of peri-implantation embryos and embryonic cells has been developed in 2D culture environment [31]. Recently, a murine 3D biomimetic culture environment was established, which could enable direct analysis of trophoblast invasion and reveal the first embryonic interactions with the maternal vasculature [32–34]. Here, we both established 3D and 2D culture environment to simulate endometrium-embryo adhesion, which consistently demonstrated a remarkable promotion effect of *L. vaginalis* metabolites (especially galangin and daidzein) on endometrial-embryonic cells adhesion. However, the complexity of the maternal environment, which consists of multiple cell types and tissue structures, cannot be

fully recapitulated *ex utero* with the current state of technology in every in vitro model [34]. Therefore, it is not only sufficient but also required to examine the improvement effects of maternal *L. vaginalis* and its metabolites supply during early gestation on embryo survival and litter performance in mice and sows.

C. butyricum is a butyrate producer that have been investigated for potential protective or ameliorative effects in a wide range of diseases, including intestinal injury and inflammatory, neurodegenerative disease, and metabolic disease [35]. Indeed, butyrate has been shown to increase mucin and defensin expression to maintain intestinal barrier function, as well as regulate energy homeostasis via G protein-coupled receptors or histone deacetylase inhibitor [36]. Interestingly, it is noteworthy that our previous studies have described the roles of butyrate in enhancing ovarian steroidogenesis and improving uterine epithelial cell receptivity, which could contribute to promote embryo implantation and survival [37–39]. In our present study, we found that the abundance of intestinal *C. butyricum* was significantly increased in sows with higher litter size. However, neither the number of embryo implantation sites nor the litter size and total litter weight was changed after *C. butyricum* transplantation in mice. It is probably because butyrate produced by *C. butyricum* that colonized at the posterior intestine colon was most utilized for intestinal epithelium cells on energy supply, and only a small part of butyrate could enter the blood circulation to stimulate the target tissues [36]. Moreover, it is also suggested that *C. butyricum* may modulate the composition of the gut microbiota, possibly increasing certain beneficial bacterial taxa including *Lactobacillus* [40]. Therefore, whether particular doses of *C. butyricum* benefit ovarian steroidogenesis and uterine receptivity to, in turn improve embryo implantation and survival through a butyrate-producing pathway or gut microbiota composition modulating is an interesting question for future study. Moreover, there may be any other microbes (both bacteria and fungi) that could affect embryo survival and litter performance in mammals, thus it needs more efforts to obtain as many as functional microbes considering the critical regulations of breed, diets, and environment on microbiota composition and activity.

In conclusion, we declared that intestinal microbial-host interactions occurred during early pregnancy, which could contribute to maternal metabolic changes and then influence pregnancy outcomes in mammals. Overall, our study demonstrated that maternal intestinal *L. vaginalis* facilitated embryo implantation and survival during early pregnancy, ultimately improved litter performance. Our study provides insights of maternal microbiota improving pregnancy outcomes through a gut-uterus axis, contributing to advanced concept and novel strategy to manipulate gut microbiota during early pregnancy, and in turn to reduce embryo loss in mammals.

Materials and methods

Bacteria culture

Clostridium butyricum (*C. butyricum*) was purchased from BeNa Culture Collection (Catalogue number: BNCC337239), and *Lactobacillus vaginalis* (*L. vaginalis*) was purchased from China Center of Industrial Culture Collection (Catalogue number: CICC6120). *C. butyricum* and *L. vaginalis* were respectively cultured in Reinforced Clostridium Medium (RCM) and de Man, Rogosa, and Sharpe (MRS) medium at 37 ℃ in an anaerobic incubator. The bacterial growth curve was measured by turbidimetric method, as previously described [41].

Cell culture

Porcine endometrial epithelial cells (PEECs, catalogue number: BFN60808569) and porcine trophoblast cells (PTCs, catalogue number: BFN60808646) were purchased from Qingqi Biotechnology Development Co., Ltd. (Shanghai, China). Porcine iliac artery endothelial cells (PIECs, catalogue number: SNL-035) were purchased from Shanen Biotechnology Development Co., Ltd. (Wuhan, China). PEECs, PTCs, and PIECs were both cultured in Dulbecco's modified Eagle's medium (DMEM) supplemented with 10% fetal bovine serum (FBS, Gibco, catalogue number: 2305262RP) and 100 IU/mL penicillin and 100 mg/mL streptomycin. Cells were washed with phosphate buffered saline (PBS) and cultured at 37 °C in a humidified 5% CO_2 incubator.

Feces collection and microbiota transplantation in sows

One hundred and sixty primiparous Landrace × Yorkshire crossbred (L × Y) sows with similar genetic background that fed in the DBN sows farm in Huangpi district, Wuhan city, Hubei province, China, were used in this study. L × Y sows were fed the fortified corn-soybean diets, which were formulated to meet or exceed National Research Council nutrient requirements. The fresh feces of sows were collected in the morning of day 28 of gestation (a period for placental development and embryonic organ formation) using sterile centrifugal tube and freezed in the liquid nitrogen immediately. Most embryo loss have occurred before or during day 28 of gestation, and the potential litter size is established at this period [42, 43]. Therefore, we collected the samples at day 28 of gestation of sows to explore the correlation between intestinal microbiome and embryo survival. After farrowing, the number of total piglets born (litter size) and the number of piglets born alive (live litter size) were recorded, and sows with litter size nearly 15 ~ 21 or 9 ~

11 were respectively grouped into High L× Y group (n = 21) or Low L× Y group (n = 21).

For microbiota transplantation in sows, 40 L× Y multiparity sows with similar genetic background and body condition were randomly assigned to 3 groups including Control group (n = 16), LV_B group (n = 12), and LV_M group (n = 12). Sows in control group did not do any experimental treatment, and sows in LV_B and LV_M groups were respectively oral administrated with 15 mL *L. vaginalis* (2×10^8 CFU/kg, excluding in vitro cultured medium and metabolites) or 15 mL in vitro cultured metabolites of *L. vaginalis* every other day from day 1 to day 28 of gestation. The metabolites of *L. vaginalis* were obtained by centrifugating bacterial solution at 8000 g for 30 min and then filtrating through a sterile filter with a pore size of 0.22 μm after *L. vaginalis* cultured for 30 h. The litter performance including total litter size, live litter size, litter size of litter pup's weight higher than 0.95 kg, total litter weight, and average litter pup's weight was recorded. The feces of sows at day 28 of gestation were collected to detect the abundance of *L. vaginalis*.

Microbiota transplantation in mice

ICR mice (aged 7 weeks, 20–25 g body weight) were housed in a temperature-controlled environment (22–25 ℃) on a 12-h-light/12-h-dark cycle with ad libitum access to granulated feed and water. After 1 week of acclimation, virgin female ICR mice had free access to drinking water supplemented with 1 mg/mL ampicillin and 1 mg/mL neomycin for 7 days. In Experiment 1, mice in group PBS, CB, LV, or CB + LV were respectively received intragastric administration of 200 μL PBS without or with 2×10^8 CFU/kg *C. butyricum* or *L. vaginalis* (containing in vitro cultured medium with metabolites) separately or in combination with equal proportions. In Experiment 2**,** mice in MRS, LV_B, and LV_M groups were respectively received intragastric administration of 200 μL PBS containing MRS medium (1:100, v/v), 2×10^8 CFU/kg *L. vaginalis* (excluding in vitro cultured medium and metabolites) or in vitro cultured metabolites (diluted in PBS with ratio of 1:100, v/v) of *L. vaginalis*. Mice in PBS group were received intragastric administration of 200 μL PBS. In Experiment 1 and Experiment 2, after three times intragastric administration during pre-breeding, pregnancy of mice was induced by overnight caging of two females with one male of proven fertility. The presence of vaginal plugs in the next morning is deemed as day 1 of pregnancy (1 dpc), and the pregnant mice were continually gavaged with corresponding probiotics every other day for three times. The numbers of embryo implantation sites in uterus and corpus luteum in ovaries, as well as the embryo implantation efficiency (the number of embryo implantation sites/the number of corpus luteum) at 6 dpc and the reproductive performance after farrowing were recorded. At 0900 ~1000 in the morning, the plasma samples were collected at 4 dpc and 6 dpc, and the ovaries, uterus, and colonic tissue and contents were obtained at 4 dpc in experiment 1.

Microbial genomic DNA extraction and 16S rRNA gene sequencing

The bacterial genomic DNA of fecal samples or intestinal contents was extracted using the protocol of the repeated bead beating plus column method with a TIANamp stool DNA kit. DNA concentrations were measured using a Nanodrop-1000 instrument, and DNA quality assessed by 0.8% agarose gel electrophoresis. The V3–V4 hypervariable region of the 16S rRNA gene was amplified with the barcode fusion primers (338 F: 5′-ACTCCTACG GGAGGCAGCAG-3′, 806R: 5′-GGACTACHVGGG TWTCTAAT-3′) as previously described [44]. The purified amplicons were pooled in equimolar amounts and paired-end sequenced on an Illumina MiSeq PE300 platform (Illumina, San Diego, USA) according to the standard protocols by Majorbio Bio-Pharm Technology Co. Ltd. (Shanghai, China). After demultiplexing, the resulting sequences were quality filtered with fastp and merged with FLASH. Then the high-quality sequences were denoised using DADA2 plugin in the Qiime2 pipeline with recommended parameters, which obtains single nucleotide resolution based on error profiles within samples. DADA2 denoised sequences are usually called amplicon sequence variants (ASVs). Bioinformatic analysis of the fecal microbiota was carried out using the Majorbio Cloud platform (https://cloud.majorbio.com).

Untargeted-metabolomics analysis

The polar metabolite profiles in feces or plasma were detected at Majorbio using liquid chromatography tandem mass spectrometry (LC–MS/MS). Briefly, 50-mg feces were weighed and then extracted using 400 μL methanol:water (4:1, v/v) solution with 0.02 mg/mL L-2-chlorophenylalanin as internal standard. Plasmas were separated from blood samples by centrifugation. The mass spectrometric data were collected using a UHPLC-Q Exactive HF-X Mass Spectrometer (Thermo Scientific, Waltham, MA) equipped with an electrospray ionization source operating in either positive or negative ion mode. The selection of significant different metabolites was determined based on the p-value of Student's t test ($p < 0.05$), the variable importance in the projection (VIP) obtained by the OPLS-DA model (VIP > 1.0), and the fold change (High L× Y vs Low L× Y) ≥ 2.0 or ≤ 0.5. Differential metabolites among two groups were mapped into biochemical pathways at MetaboAnalyst (https://

www.metaboanalyst.ca/) based on Kyoto Encyclopedia of Genes and Genomes (KEGG) database.

Quantification of SCFAs profiling

SCFAs in feces were quantified with gas chromatography. Briefly, 1 g of feces were weighted, dissolved and homogenized in 1 mL methanol. Then, the homogenized solution was centrifuged at 12,000 g for 10 min at 4 °C to obtain the supernatant that transferred into a new tube. The supernatant was diluted (5:1, v/v) with 25% metaphosphoric acid at 4 °C overnight and then centrifuged at 12,000 g for 10 min at 4 °C. Finally, the supernatant was subjected for SCFAs analysis with a gas chromatography following a previously published protocol [45].

Measurement of steroid hormones

Steroid hormones including estradiol and progesterone in feces were measured using commercially available radioimmunoassay kits (Beijing North Institute of Biotechnology). Briefly, 0.2 g of fecal samples were weighted, dissolved and homogenized in 1 mL 80% ethanol. After incubation at 70 °C for 15 min and vortex for 1 min, the homogenized solution was centrifuged at 4000 rpm for 15 min at 4 °C to obtain the supernatant. Then, 0.5 mL 80% ethanol was added into the residue and vortex for 1 min, followed by centrifuging at 4000 rpm for 15 min at 4 °C to merge the supernatant. The supernatant was dried in a vacuum concentrator using nitrogen, and the residue was re-dissolved in phosphate buffer to detect the estradiol or progesterone levels using iodine [^{125}I] estradiol radioimmunoassay kit or iodine [^{125}I] progesterone radioimmunoassay kit with a modification of the previous method [38].

Transcriptome analysis

Total RNA of uterine tissues of mice at day 4 of pregnancy was isolated using TRIzol and sent for library preparation and sequencing by Majorbio Biotech using Illumina Hiseq 2000. The reads count for each gene in each sample was counted, and fragments per kilobase million mapped reads (FPKM) was then calculated to estimate the expression level of genes. DEGseq was used for differential gene expression analysis, and the significant different expressed genes (DEGs) were filtered with p value <0.05 and fold change >2.0 or <0.5. The DEGs were enriched to GO terms, and a network plot was used to show the subset of enriched clusters on Metascape (https://www.metascape.org). Also, the biological pathways were analyzed using Gene Set Enrichment Analysis (GSEA) based on KEGG database.

Hematoxylin and eosin (H&E) staining

Uterine and colonic tissues of mice at day 6 of pregnancy were collected and preserved in 4% paraformaldehyde overnight. Then, tissues were embedded in paraffin wax following immersion in a graded series of alcohols (70–100%) and sectioned (5 mm) and dried at 56 °C for 24 h. The slides were passed through a series of the clearing agent xylene and rehydrated in a graded series of ethanol and wash in distilled water, followed by incubating with hematoxylin solution and washing with running tap water. Next, the sections were differentiated in 1% acid alcohol and washed with running tap water, followed by an incubation in eosin counterstain and dehydration in a graded series of ethanol and immersion in xylene.

Metabolites detection of *L. vaginalis*

The metabolites of *L. vaginalis* were detected by high-throughput targeted metabolomics analysis using ultra performance liquid chromatography-mass spectrometry (UPLC-MS) at Beijing Genomics Institute (BGI). Briefly, the medium of *L. vaginalis* after in vitro cultured for 0, 4, 12, and 30 h were collected and filtered through a sterile filter with a pore size of 0.22 μm. Then, the extraction agent (methanol:acetonitrile:water =4:2:1, v/v/v) contained interior label was added into samples, followed by vortex and centrifugation to obtain the supernatant, which was transformed into a 96-well plate and added derivatization reagent and EDC working reagent in turn. After incubation of the 96-well plate in a thermostatic oscillator for 60 min at 1200 rpm and 30 ℃, pre-cooled methanol:water (1:1, v/v) was added and centrifugated to obtain the supernatant, which was transferred to the microporous plate pre-loaded with the internal standard II working liquid. The column was used BEH C18 (2.1 mm ×10 cm, 1.7 μm, waters), and the sample extracts were analyzed using Waters UPLC I-Class Plus (Waters, USA) equipped with QTRAP 6500 Plus (SCIEX, USA).

RNA isolation and qRT-PCR analysis

The gene expression levels related to endometrial epithelium receptivity were detected after different doses of *L. vaginalis* metabolites including galangin (MedChemExpress, catalogue number: HY-N0382), norethindrone (MedChemExpress, catalogue number: HY-N0554), TCA (MedChemExpress, catalogue number: HY-N0545), daidzein (MedChemExpress, catalogue number: HY-N0019), or caproic acid (Sigma-Aldrich, catalogue number: 153745) treatment for 24 h in PEECs. The gene expression levels related to ovarian steroid hormones synthesis were also detected after *L. vaginalis* gavage in mice at day 4 and day 6 of pregnancy. Primers were designed using Primer 3.0 and shown in Table S1. The RNA of PEEC cells

or entire unilateral ovarian tissue of mice were isolated using RNAiso Plus. The quality and quantity of RNA were respectively evaluated by gel electrophoresis and NanoDrop spectrophotometer. qRT-PCR was conducted on an Applied Biosystems 7500 qPCR System (Applied Biosystems) using gene-specific primer pairs to amplify target cDNA segments with the SYBR Premix EX Taq kit.

Fabrication of a porcine endometrium-on-a-chip model

A porcine endometrium-on-a-chip model was established by co-culturing PEECs and PIECs within a microfluidic hydrogel scaffold, aiming to mimic the endometrial epithelium and blood vessels of the porcine uterus. In brief, digital light processing 3D printing was used to fabricate the master molds for the microfluidic chip and rods. Polydimethylsiloxane (PDMS) was applied to the masters at a ratio of 10:1 base to curing agent and allowed to polymerize for 5 h at 70 °C. Following curing, the PDMS chip was demolded, and four through holes were punched on the walls between each medium reservoir and main chamber. The inner surface of the main chamber underwent a coating process with 1% polyethyleneimine for 10 min and 0.1% glutaraldehyde for 30 min to enhance collagen adhesion. Two PDMS rods (600 μm in diameter) were inserted through the holes in the chip, and a solution of bovine dermis collagen precursor (4 mg/mL) was loaded into the main chamber. The collagen gel was allowed to polymerize in a 37 °C incubator for 0.5 h. Subsequently, the PDMS rods were carefully removed with tweezers, creating hollow channels within the hydrogel scaffold.

A suspension of PIECs at a density of 1×10^6 cells/mL was injected into the hollow channels and incubated for 30 min, allowing the endothelial cells to settle by gravity and attach to the lower surface of the channels. This process was repeated with flipping the chip at 180 ℃, promoting cells adhesion to the opposite surface of the channel. Following the attachment of PIECs, PEECs at a density of 5×10^5/mL was loaded to the chamber above the hydrogel scaffold and allowed to adhere to the hydrogel surface for 30 min. Subsequently, cell culture medium was introduced into the top chamber and four reservoirs. The chip was cultured in a 37 °C incubator.

Cell adhesion assay and cell surface morphology

The cell adhesion assay to simulate endometrium-embryo adhesion was conducted by detecting the adhesiveness of PTCs to endometrial microfluidic chip. After treatments of *L. vaginalis* metabolites including galangin (5 μM), norethindrone (1 μM), TCA (10 μM), daidzein (20 μM), or caproic acid (100 μM) for 24 h in PEECs, PTCs pre-stained with Hoechst for 1 h were suspended and equivolumetrically seeded onto endometrial microfluidic chip to co-culture for 1 h at 37 °C. The unattached PTCs were removed by washing with PBS for three times, and the images were taken with a fluorescence microscope. In addition, the microvilli and pinopode on cell surface of PEECs were observed using a scanning electron microscope after treatments of *L. vaginalis* metabolites including galangin (5 μM), norethindrone (1 μM), TCA (10 μM), daidzein (20 μM), or caproic acid (100 μM) for 24 h.

Quantification and statistical analysis

Data were presented as means ± SEM. Figures were prepared with GraphPad Prism 9 or R v4.0.2. Statistical comparisons were analyzed using non-paired Student's *t*-test (for comparisons between two groups that coincide with normal distribution), Mann–Whitney *U* test (for comparisons between two groups that do not coincide with normal distribution), or one-way ANOVA with Dunnett correction test (for comparisons among more than two groups with one variable). For non-paired Student's *t*-test and Mann–Whitney *U* test, differences were considered statistically significant if $^*p < 0.05$ or $^{**}p < 0.01$. For one-way ANOVA, differences were considered statistically significant if $p < 0.05$ and represented as mean values without a common letter.

Supplementary Information

The online version contains supplementary material available at https://doi.org/10.1186/s40168-025-02141-7.

Additional file 1. Supplemental information includes four figures and one table.

Acknowledgements

We thank Yan lab's members for helpful discussions and critical reading of the manuscript.

Authors' contributions

Q.H.Y. and X.H.Y. designed the research. Q.H.Y., Y.F.H., T.T.L., L.S.H., H.Y.J., Y.W.C., J.Y.C. and L.B.M. performed the research. Q.H.Y., Z.Y.H. and X.H.Y. analyzed the data. Q.H.Y. wrote the paper and X.H.Y. revised the paper with the help of all authors. All authors read and approved the final version of the manuscript.

Funding

This work was supported by the National Natural Science Foundation of China (32230099, 31925037 and 32202700), the National Key R&D Program of China (2022YFD1300405), the National Key Laboratory of Agricultural Microbiology (AML2023B06), Knowledge Innovation Program of Wuhan-Shuguang Project (2022020801020232), and the Fundamental Research Funds for the Central University (2662023DKPY002).

Data availability

The raw data of 16S rRNA sequencing and transcriptome used in this study are available on NCBI SRA with accession number PRJNA1055675 and PRJNA1056047.

Declarations

Ethics approval and consent to participate

All experiments were conducted with the approval of the Institutional Animal Care and Use Committee of Huazhong Agricultural University (Approval number: 202311010004 and 202401210006), in accordance with the governmental regulations of China.

Consent for publication
Not applicable.

Competing interests
The authors declare no competing interests.

Author details
[1]National Key Laboratory of Agricultural Microbiology, Frontiers Science Center for Animal Breeding and Sustainable Production, Hubei Hongshan Laboratory, College of Animal Sciences and Technology, Huazhong Agricultural University, Wuhan 430070, Hubei, China. [2]The Cooperative Innovation Center for Sustainable Pig Production, Wuhan 430070, Hubei, China. [3]Hubei Provincial Engineering Laboratory for Pig Precision Feeding and Feed Safety Technology, Wuhan 430070, Hubei, China. [4]National Engineering Research Center for Green Feed and Healthy Breeding, Key Laboratory of Animal Molecular Nutrition, Ministry of Education, Key Laboratory of Animal Nutrition and Feed Science (Eastern of China), Ministry of Agriculture and Rural Affairs, Zhejiang Key Laboratory of Nutrition and Breeding for High-quality Animal Products Institute of Feed Science, College of Animal Science, Zhejiang University, Zhejiang 310058 Hangzhou, China.

Received: 16 May 2024 Accepted: 12 May 2025
Published online: 18 June 2025

References

1. Ogawa S, Takahashi H, Satoh M. Genetic parameter estimation for pork production and litter performance traits of Landrace, Large White, and Duroc pigs in Japan. J Anim Breed Genet. 2023;140:607–23.
2. Kimura I, Miyamoto J, Ohue-Kitano R, Watanabe K, Yamada T, Onuki M, Aoki R, Isobe Y, Kashihara D, Inoue D, et al. Maternal gut microbiota in pregnancy influences offspring metabolic phenotype in mice. Science. 2020;367:eaaw8429.
3. Ye Q, Zeng X, Cai S, Qiao S, Zeng X. Mechanisms of lipid metabolism in uterine receptivity and embryo development. Trends Endocrinol Metab. 2021;32:1015–30.
4. Norwitz ER, Schust DJ, Fisher SJ. Implantation and the survival of early pregnancy. N Engl J Med. 2001;345:1400–8.
5. Ye X. Uterine luminal epithelium as the transient gateway for embryo implantation. Trends Endocrinol Metab. 2020;31:165–80.
6. Ye X, Hama K, Contos JJ, Anliker B, Inoue A, Skinner MK, Suzuki H, Amano T, Kennedy G, Arai H, et al. LPA3-mediated lysophosphatidic acid signalling in embryo implantation and spacing. Nature. 2005;435:104–8.
7. Lessey BA, Young SL. What exactly is endometrial receptivity? Fertil Steril. 2019;111:611–7.
8. Macpherson AJ, de Agüero MG, Ganal-Vonarburg SC. How nutrition and the maternal microbiota shape the neonatal immune system. Nat Rev Immunol. 2017;17:508–17.
9. Dai Z, Wu Z, Hang S, Zhu W, Wu G. Amino acid metabolism in intestinal bacteria and its potential implications for mammalian reproduction. Mol Hum Reprod. 2015;21:389–409.
10. Gill SR, Pop M, Deboy RT, Eckburg PB, Turnbaugh PJ, Samuel BS, Gordon JI, Relman DA, Fraser-Liggett CM, Nelson KE. Metagenomic analysis of the human distal gut microbiome. Science. 2006;312:1355–9.
11. Qi X, Yun C, Pang Y, Qiao J. The impact of the gut microbiota on the reproductive and metabolic endocrine system. Gut Microbes. 2021;13:1–21.
12. Vuong HE, Pronovost GN, Williams DW, Coley EJL, Siegler EL, Qiu A, Kazantsev M, Wilson CJ, Rendon T, Hsiao EY. The maternal microbiome modulates fetal neurodevelopment in mice. Nature. 2020;586:281–6.
13. Qi X, Yun C, Sun L, Xia J, Wu Q, Wang Y, Wang L, Zhang Y, Liang X, Wang L, et al. Gut microbiota-bile acid-interleukin-22 axis orchestrates polycystic ovary syndrome. Nat Med. 2019;25:1225–33.
14. Thorburn AN, McKenzie CI, Shen S, Stanley D, Macia L, Mason LJ, Roberts LK, Wong CH, Shim R, Robert R, et al. Evidence that asthma is a developmental origin disease influenced by maternal diet and bacterial metabolites. Nat Commun. 2015;6:7320.
15. Ford SP, Vonnahme KA, Wilson ME. Uterine capacity in the pig reflects a combination of uterine environment and conceptus genotype effects. J Anim Sci. 2002;80:E66–73.
16. Zhang S, Lin H, Kong S, Wang S, Wang H, Wang H, Armant DR. Physiological and molecular determinants of embryo implantation. Mol Aspects Med. 2013;34:939–80.
17. Cha J, Sun X, Dey SK. Mechanisms of implantation: strategies for successful pregnancy. Nat Med. 2012;18:1754–67.
18. Koren O, Goodrich JK, Cullender TC, Spor A, Laitinen K, Bäckhed HK, Gonzalez A, Werner JJ, Angenent LT, Knight R, et al. Host remodeling of the gut microbiome and metabolic changes during pregnancy. Cell. 2012;150:470–80.
19. Husso A, Pessa-Morikawa T, Koistinen VM, Kärkkäinen O, Kwon HN, Lahti L, Iivanainen A, Hanhineva K, Niku M. Impacts of maternal microbiota and microbial metabolites on fetal intestine, brain, and placenta. BMC Biol. 2023;21:207.
20. Ganal-Vonarburg SC, Hornef MW, Macpherson AJ. Microbial-host molecular exchange and its functional consequences in early mammalian life. Science. 2020;368:604–7.
21. Shao Y, Zhou J, Xiong X, Zou L, Kong X, Tan B, Yin Y. Differences in gut microbial and serum biochemical indices between sows with different productive capacities during perinatal period. Front Microbiol. 2020;10:3047.
22. Elovitz MA, Gajer P, Riis V, Brown AG, Humphrys MS, Holm JB, Ravel J. Cervicovaginal microbiota and local immune response modulate the risk of spontaneous preterm delivery. Nat Commun. 2019;10:1305.
23. Fettweis JM, Serrano MG, Brooks JP, Edwards DJ, Girerd PH, Parikh HI, Huang B, Arodz TJ, Edupuganti L, Glascock AL, et al. The vaginal microbiome and preterm birth. Nat Med. 2019;25:1012–21.
24. Hillier SL, Nugent RP, Eschenbach DA, Krohn MA, Gibbs RS, Martin DH, Cotch MF, Edelman R, Pastorek JG 2nd, Rao AV, et al. Association between bacterial vaginosis and preterm delivery of a low-birth-weight infant. N Engl J Med. 1995;333:1737–42.
25. Low N, Chersich MF, Schmidlin K, Egger M, Francis SC, van de Wijgert JH, Hayes RJ, Baeten JM, Brown J, Delany-Moretlwe S, et al. Intravaginal practices, bacterial vaginosis, and HIV infection in women: individual participant data meta-analysis. PLoS Med. 2011;8:e1000416.
26. Delgado-Diaz DJ, Jesaveluk B, Hayward JA, Tyssen D, Alisoltani A, Potgieter M, Bell L, Ross E, Iranzadeh A, Allali I, et al. Lactic acid from vaginal microbiota enhances cervicovaginal epithelial barrier integrity by promoting tight junction protein expression. Microbiome. 2022;10:141.
27. Giordani B, Parolin C, Abruzzo A, Foschi C, Marangoni A, Luppi B, Vitali B. Limosilactobacillus vaginalis exerts bifidogenic effects: a novel postbiotic strategy for infant prebiotic supplementation. Nutrients. 2023;15:4433.
28 Dempsey E, Corr SC. Lactobacillus spp. for gastrointestinal health: current and future perspectives. Front Immunol. 2022;13:840245.
29. Zeng Y, Wu R, Wang F, Li S, Li L, Li Y, Qin P, Wei M, Yang J, Wu J, et al. Liberation of daidzein by gut microbial β-galactosidase suppresses acetaminophen-induced hepatotoxicity in mice. Cell Host Microbe. 2023;31:766–80.
30. Tian M, Chen J, Liu J, Chen F, Guan W, Zhang S. Dietary fiber and microbiota interaction regulates sow metabolism and reproductive performance. Anim Nutr. 2020;6:397–403.
31. Morris SA, Grewal S, Barrios F, Patankar SN, Strauss B, Buttery L, Alexander M, Shakesheff KM, Zernicka-Goetz M. Dynamics of anterior-posterior axis formation in the developing mouse embryo. Nat Commun. 2012;3:673.
32. Ichikawa T, Zhang HT, Panavaite L, Erzberger A, Fabrèges D, Snajder R, Wolny A, Korotkevich E, Tsuchida-Straeten N, Hufnagel L, et al. An ex vivo system to study cellular dynamics underlying mouse peri-implantation development. Dev Cell. 2022;57:373–86.
33. Bondarenko V, Nikolaev M, Kromm D, Belousov R, Wolny A, Blotenburg M, Zeller P, Rezakhani S, Hugger J, Uhlmann V, et al. Embryo-uterine interaction coordinates mouse embryogenesis during implantation. Embo J. 2023;42:e113280.
34. Govindasamy N, Long H, Jeong HW, Raman R, Özcifci B, Probst S, Arnold SJ, Riehemann K, Ranga A, Adams RH, et al. 3D biomimetic platform reveals the first interactions of the embryo and the maternal blood vessels. Dev Cell. 2021;56:3276–87.
35. Stoeva MK, Garcia-So J, Justice N, Myers J, Tyagi S, Nemchek M, McMurdie PJ, Kolterman O, Eid J. Butyrate-producing human gut symbiont, clostridium butyricum, and its role in health and disease. Gut Microbes. 2021;13:1–28.
36. Zhang L, Liu C, Jiang Q, Yin Y. Butyrate in energy metabolism: there is still more to learn. Trends Endocrinol Metab. 2021;32:159–69.

37. Ye Q, Li H, Xu B, He Z, Yan X. Butyrate improves porcine endometrial epithelial cell receptivity via enhancing acetylation of histone H3K9. Mol Nutr Food Res. 2023;67:e2200703.
38. Ye Q, Zeng X, Wang S, Zeng X, Yang G, Ye C, Cai S, Chen M, Li S, Qiao S. Butyrate drives the acetylation of histone H3K9 to activate steroidogenesis through PPARγ and PGC1α pathways in ovarian granulosa cells. FASEB J. 2021;35:e21316.
39. Ye Q, Cai S, Wang S, Zeng X, Ye C, Chen M, Zeng X, Qiao S. Maternal short and medium chain fatty acids supply during early pregnancy improves embryo survival through enhancing progesterone synthesis in rats. J Nutr Biochem. 2019;69:98–107.
40. Pan LL, Niu W, Fang X, Liang W, Li H, Chen W, Zhang H, Bhatia M, Sun J. Clostridium butyricum strains suppress experimental acute pancreatitis by maintaining intestinal homeostasis. Mol Nutr Food Res. 2019;63:e1801419.
41. Li RC, Nix DE, Schentag JJ. New turbidimetric assay for quantitation of viable bacterial densities. Antimicrob Agents Chemother. 1993;37:371–4.
42. Lyderik KK, Østrup E, Bruun TS, Amdi C, Strathe AV. Fetal and placental development in early gestation of hyper-prolific sows. Theriogenology. 2023;197:259–66.
43. Langendijk P. Latest advances in sow nutrition during early gestation. Animals. 2021;11:1720.
44. Yang H, Wu J, Huang X, Zhou Y, Zhang Y, Liu M, Liu Q, Ke S, He M, Fu H, et al. ABO genotype alters the gut microbiota by regulating GalNAc levels in pigs. Nature. 2022;606:358–67.
45. Fellows R, Denizot J, Stellato C, Cuomo A, Jain P, Stoyanova E, Balázsi S, Hajnády Z, Liebert A, Kazakevych J, et al. Microbiota derived short chain fatty acids promote histone crotonylation in the colon through histone deacetylases. Nat Commun. 2018;9:105.

Publisher's Note